JOURNAL OF INFORMATION SCIENCE AND ENGINEERING 23, 1421-1436 (2007)

Design of Force-Reflection Joystick System for VR-Based Simulation*

WEI-CHING LIN+ AND KUU-YOUNG YOUNG
+*Chung-shan Institute of Science and Technology*
Taoyuan, 325 Taiwan
Department of Electrical and Control Engineering
National Chiao Tung University
Hsinchu, 300 Taiwan

In this paper, we develop a force-reflection joystick system for VR-based simulation, including a 2-DOF joystick and the related software. The developed force-reflection joystick, as a kind of haptic device, provides two-way communication in both position and force, and is very helpful for the user to interact with a simulation system. By considering the main factors in designing a force-reflection joystick, we build the joystick to be with the bandwidth, precision, and output torque comparable to the advanced commercial joystick. We also perform workspace analysis, system identification, and system modeling to better connect the joystick with the simulation system. To make it suitable for various applications, the software is developed to generate virtual motion constraints, so that the joystick is confined to operate within the workspace that corresponds to task requirements. In other words, the joystick may behave like a manipulative device specific for the given task. For demonstration, in experiments, we use the developed joystick system to emulate a virtual manual gearshift system.

Keywords: force-reflection joystick, virtual motion constraint, simulation system, haptic device, virtual reality

1. INTRODUCTION

Along with rapid progress in dynamic modeling and virtual reality (VR) techniques, the simulation system now can generate realistic simulated environment and communicate with the user via various channels [1-5]. To enhance bilateral interaction between the user and simulation system, the haptic devices are introduced to provide both position and force information. Various kinds of haptic devices have been developed, such as data glove, force-reflection joystick, and pen-based and robot-based haptic interfaces [6]. Among them, the force-reflection joystick has the merit in its simplicity and generality. However, since the joystick may be used to manipulate various types of mechanisms in different applications, it may not be fully compatible with each of the manipulated mechanisms, which may lead to unnatural manipulation. To tackle this incompatibility, the concepts of virtual mechanism and virtual fixture previously proposed may be helpful. The idea is to generate virtual motion constraints via the software, so that the joystick is con-

Received August 22, 2005; revised November 23, 2005 & August 10, 2006; accepted November 1, 2006.
Communicated by Chin-Teng Lin.
* Part of this paper has been presented at International Conference on Mechatronics Technology, Taipei, Taiwan, 2003. This work was supported in part by the National Science Council of Taiwan, under grant No. NSC 94-2218-E-009-006, and also by Department of Industrial Technology under grant No. 94-EC-17-A-02-S1-032.

strained to move within a limited workspace that corresponds to task requirements [7, 8]. In other words, the user may feel she/he is operating a joystick that is specifically designed for the given task, thus achieving fast and effective manipulation. Motivated by this idea, in this paper, we develop a 2-DOF force-reflection joystick for the VR-based simulation system, along with the software for building virtual motion constraints.

In designing this force-reflection joystick, we first study its major components, including the transmission mechanism, actuator, and sensor [9, 10]. Their performance determines the manipulability, resolution, and quality of the joystick. To meet the requirements demanded in dynamic simulations, we build the joystick to be with the bandwidth, precision, and output torque comparable to the famous Immersion engine 2000, an advanced commercial joystick from the Immersion Corporation. We also perform workspace analysis and system identification, and then system modeling. With the joystick well modeled, the integration between the joystick and simulation system can be much enhanced and salient collaboration between them be achieved.

In software development, we first install the physical properties into the program, and let the joystick emulate the three basic physical elements, the spring, damper, and mass. Objects with more complex behaviors can be emulated by synthesizing these three basic elements. We then implement the virtual wall to serve as the building block for constructing various virtual motion constraints. A set of horizontal and vertical walls are built and transition rules for governing movements between walls established. Thus, by properly assembling the virtual walls, virtual motion constraints that correspond to task requirements can be generated. In other words, with the developed 2-DOF force-reflection joystick and the set of virtual walls, various types of virtual mechanisms and manipulative devices can be constructed. As a demonstration, we build a virtual manual gearshift system, in which the 2-DOF force-reflection joystick behaves just like a gearshift lever [11]. The rest of this paper is organized as follows. Section 2 describes the design and analysis of the developed 2-DOF force-reflection joystick, including its system identification and evaluation. Section 3 discusses the software development of the joystick system, including the construction of the virtual wall and virtual motion constraints. In section 4, experiments are performed to demonstrate the performance of the developed joystick system in emulating the virtual wall and manual gearshift system. Conclusions are given in section 5.

2. DESIGN AND ANALYSIS

A force-reflection joystick consists of three major components: transmission mechanism, actuator, and sensor. The structure of the transmission mechanism determines its workspace, the actuator supplies the power, and the sensor detects system states and interactions with environments. The transmission mechanism and actuator together determine the manipulability, while the resolutions of the actuator and sensor specify that of the joystick. During the design process, we first evaluate current developments of these three components and then proceed with our design, discussed in sections 2.1 to 2.3, respectively. When the hardware implementation of the whole joystick system is completed, we then perform system identification, discussed in section 2.4. As an evaluation, we compare the developed joystick system with those commercial ones, also discussed in section 2.4.

2.1 Transmission Mechanism

The design of the transmission mechanism for the 2-DOF force-reflection joystick should achieve a large workspace of the joystick at less expense of the action space of the transmission mechanism. The transmission mechanism in general can be classified as the coupled and decoupled types. For the coupled type, the mandrels (for direct transmission) or connectors (for indirect transmission), illustrated in Table 1, are used to move the joints and their movements may affect each other; while the joint movements are independent for the decoupled one, and the joints can be designed, separately. Via evaluation, our design is set to be based on the two-dimensional indirect-transmission mechanism with the single-yoke rigid connector, as shown in Fig. 1 (a) [12]. Its corresponding action space and workspace are shown in Fig. 1 (b). This design, however, has a drawback in that the two semi-circular connectors may interfere with each other when the central yoke moves around. To resolve it, we substitute one semi-circular connector by a long rectangular one and fix the yoke to be in the center of the rectangular connector, as shown in Fig. 2 (a). This modification much alleviates the interference and also friction between the two connectors, since the contact between them is eliminated.

Table 1. Classification of the coupled types of transmission mechanisms.

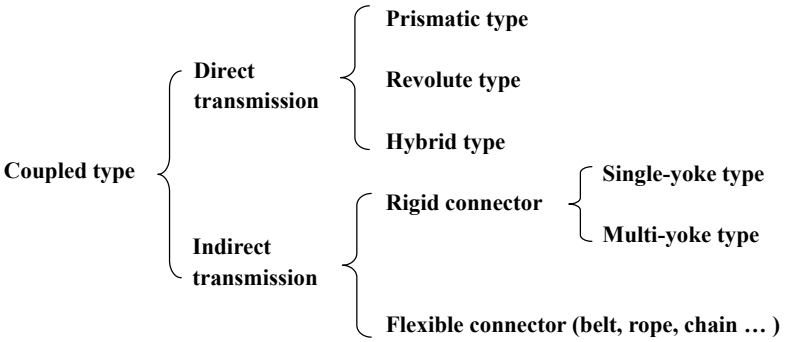

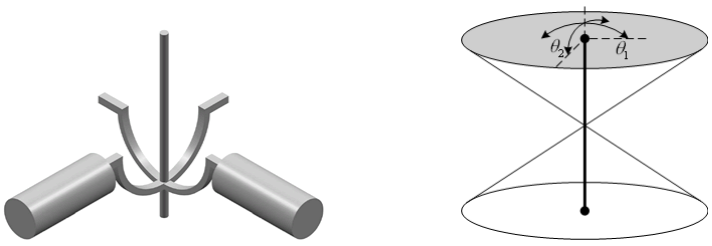

(a) Mechanism. (b) Action space and workspace.

Fig. 1. (a) The two-dimensional indirect-transmission mechanism with the single-joke rigid connector and (b) its corresponding action space and workspace.

The workspace of this modified single-yoke transmission mechanism is analyzed as follows. Fig. 2 (b) shows the movements of its two axes and Fig. 2 (c) the corresponding

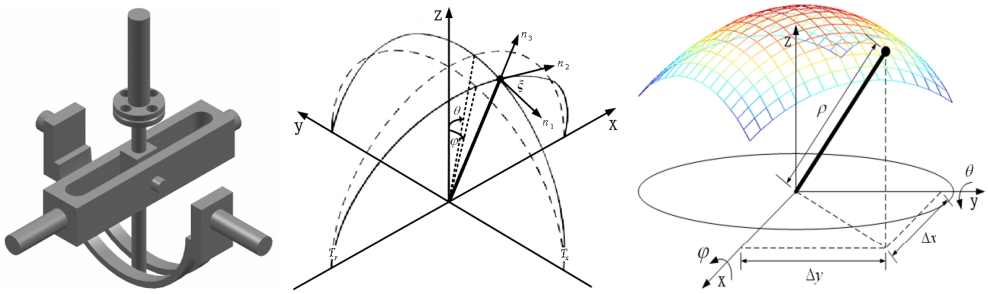

(a) Modified mechanism. (b) Axis movement. (c) Workspace.

Fig. 2. Mechanism analysis of the developed force-reflection joystick.

workspace. In Figs. 2 (b) and (c), the origin of the coordinate system is set at the center of the mechanism, ρ is the distance from the origin to the tip of the yoke, and φ and θ are the rotation angles in the X and Y directions, respectively. The rotation about the X axis will move the yoke along n_1 and form the trajectory T_x, and that about the Y axis move it along n_2 and form T_y, as shown in Fig. 2 (b). The intersection of T_x and T_y determines the location of the yoke, which points to the direction of n_3. n_3 can be obtained as the cross product of n_1 and n_2:

$$n_3 = n_1 \times n_2 = \frac{\cos\varphi \sin\theta}{\sqrt{1-\sin^2\varphi \sin^2\theta}} i - \frac{\sin\varphi \cos\theta}{\sqrt{1-\sin^2\varphi \sin^2\theta}} j + \frac{\cos\varphi \cos\theta}{\sqrt{1-\sin^2\varphi \sin^2\theta}} k \quad (1)$$

where $\varphi \in [-35°, 35°]$ and $\theta \in [-40°, 40°]$ are the operating ranges of the designed transmission mechanism. In Fig. 2 (c), the tip of the yoke on the workspace, represented by point **p**, can be described as

$$\mathbf{p} = \begin{bmatrix} p_x \\ p_y \\ p_z \end{bmatrix} = \frac{\rho}{\sqrt{1-\sin^2\varphi \sin^2\theta}} \cdot \begin{bmatrix} \cos\varphi \sin\theta \\ -\sin\varphi \sin\theta \\ \cos\varphi \cos\theta \end{bmatrix}. \quad (2)$$

When φ and θ are small, **p** can be approximated as

$$\mathbf{p} \approx \rho \cdot \begin{bmatrix} \theta \\ -\varphi \\ 1 \end{bmatrix}. \quad (3)$$

In this case, the yoke may move on a plane-like workspace, and its movement is decoupled into those of φ and θ, separately, letting the user manipulate the joystick in a more intuitive manner.

2.2 Actuator

The actuator of a force-reflection joystick is not only used to send out the commanded force to the simulation system, but also feedback the reflected force from the

interacting environment. To enhance this bilateral interaction between the user and the joystick, we did not use the gear or wire to raise the force and speed in designing the actuator, because it may affect the backdriving ability and induce discontinuous feeling. Instead, to simplify force transfer and system analysis, the AC servo motor is used as the actuator to move the joystick directly. The motor (type MSMA041A1E, manufactured by Panasonic, Japan) weighs 1.6 kg with a maximum speed of 4500 rpm and maximum output torque of 3.8 N/m. An encoder is installed within the motor to achieve closed-loop servo control with a resolution of 2500 P/r. The encoder is used to measure the position of the joystick, and a force sensor installed outside of the actuator, discussed in section 2.3, to measure the force imposed on the joystick. The resolutions of the encoder and force sensor, and the quality of the actuator's servo control altogether determine the resolution of the joystick. Because both the user's hand and the actuator may impose forces on the joystick, this combined force f_j is computed as

$$f_j = f_h - f_a \tag{4}$$

where f_h is the force exerted by the user's hand and f_a that by the actuator. f_a, generated by the torques from the actuators, τ_φ and τ_θ, corresponding to φ and θ, respectively, can be described as

$$f_a = \begin{bmatrix} f_{ax} \\ f_{ay} \end{bmatrix} = \frac{\sqrt{1-\sin^2\varphi\sin^2\theta}}{\rho} \cdot \begin{bmatrix} \frac{\tau_\theta \cos\theta}{\sin\varphi} \\ \frac{\tau_\varphi \cos\varphi}{\cos\theta} \end{bmatrix} \tag{5}$$

where the length of the yoke ρ is about 120 mm. When φ and θ are small, f_a can be approximated as

$$f_a \approx \frac{1}{\rho} \cdot \begin{bmatrix} \tau_\theta \\ -\tau_\varphi \end{bmatrix}. \tag{6}$$

From f_j, f_h, and f_a, we can evaluate how the force flows between the user and the joystick.

2.3 Sensor

We adopted the JR3 force-moment sensor (type UFS-3012A-25, manufactured by NITTA, Japan), as the force sensor. Only force measurement is used in this joystick system, and the listed maximum loads from the company are 22, 22, and 44 *kgf* in the X, Y, and Z directions, respectively, and sensitivities, 0.044, 0.044, and 0.088 *kgf*. To ensure the accuracy and find out the mapping between the actual exerted force f_e and sensor reading f_s, we performed a series of tests to find out how the sensor responded under various exerted forces in various contact directions. No load, and six standard counterpoises with weights of 100, 200, 300, 500, 750, and 1000 *g*, were used to exert forces on the eight directions uniformly distributed on the X-Y plane spanned by the X and Y axes. Results show that the sensor presented consistent readings in all those directions for tests under the same exerted forces and linearly proportional readings along with the increase

of the exerted forces in the same direction, indicating that this force sensor was quite accurate. And, the mapping between f_e and f_s (unit *gw*) was found to be

$$f_e = \frac{f_s - 19.04}{0.1551}. \tag{7}$$

2.4 System Identification and Evaluation

Fig. 3 shows the system view of the 2-DOF force-reflection joystick system developed in our laboratory. In Fig. 3, the main body of the joystick consists of the transmission mechanism, actuator, and two kinds of handles. The user can operate the joystick to generate position and force commands. These commands, sensed by the sensors, are then sent to the control card. The control card, which links the joystick system with the simulation system, modulates the commands via the installed control strategies and generates suitable signals sent to the simulation system. Meanwhile, it also receives signals from the simulation system and derives corresponding torques to push back the joystick via the driver, thus achieving bilateral interaction. With the hardware implementation completed, we then perform its system identification using the frequency-response analysis [13].

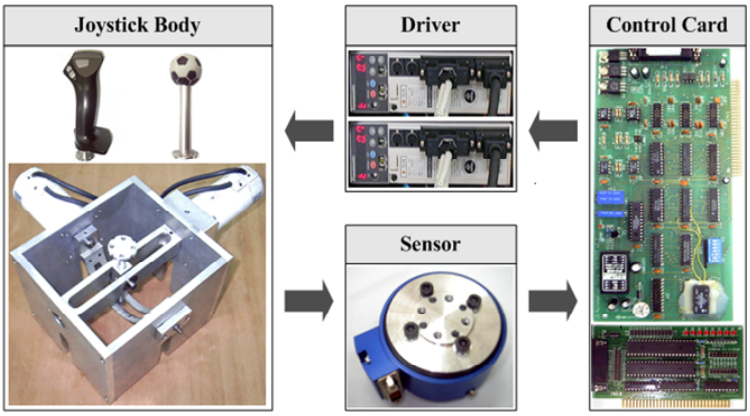

Fig. 3. System view of the 2-DOF force-reflection joystick system developed in our laboratory.

We first define the transfer function for each axis of the joystick $G(S)$ as

$$G(s) = \frac{X(s)}{F(s)} = \frac{1}{ms^2 + bs + k} \tag{8}$$

where $X(s)$ is derived from the reading of the joystick encoder, $F(s)$ the force command, and m, b, and k the parameters for the simple second-order system describing the actuator dynamics. In performing the frequency-response analysis, we input into the system a number of sinusoids $u(t)$ with various frequencies:

$$u(t) = \alpha \cos \omega t \tag{9}$$

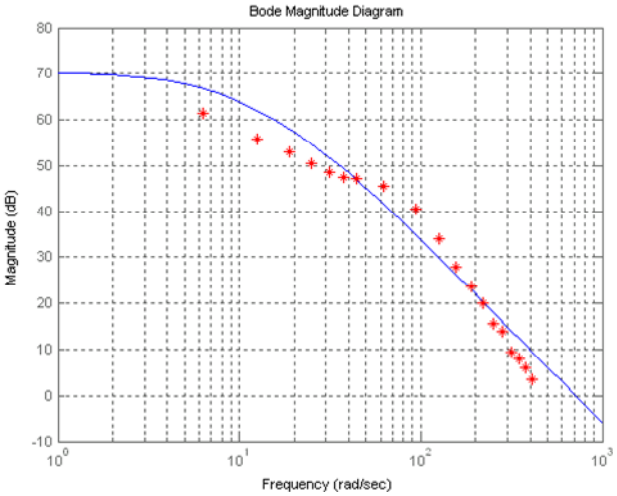

(a) X-axis bode diagram.

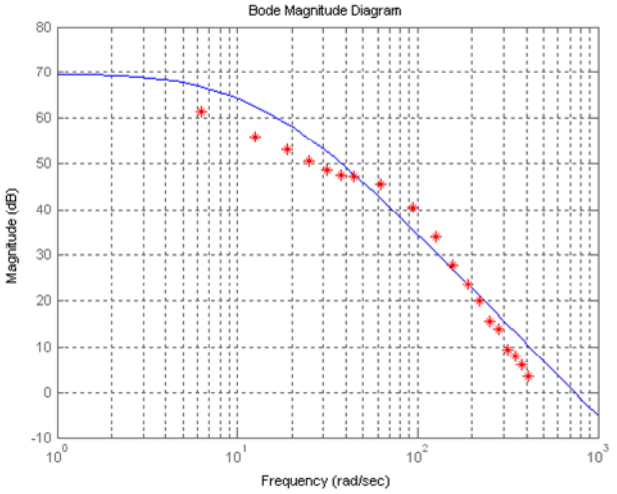

(b) Y-axis bode diagram.

Fig. 4. System identification for the 2-DOF force-reflection joystick.

where α is the amplitude, set to be one-third of the maximum output torque, and ω the frequency. The output $y(t)$ will then be

$$y(t) = \alpha|G(j\omega)|\cos(\omega t + \phi) + n(t) \tag{10}$$

where $\phi = \arg\{G(j\omega)\}$ is the phase lag and $n(t)$ the noise. During the process, the output response reached 3 dB when the input frequency was raised to about 65 Hz; we thus stopped increasing the frequency. Fig. 4 shows the Bode diagrams for the frequency responses in both the X and Y-axes, with the test points marked by the * signs. Via approximation, the transfer functions for the X and Y-axes, $G_x(s)$ and $G_y(s)$, can be estimated as

Table 2. Comparison of the immersion engine 2000, the SideWinder force Feedback Pro, and the developed force-reflection joystick.

Item		Developed	SideWinder	Immersion Engine 2000
Range (θ)	X axis	70 ~ 80 deg	45 ~ 55 deg	65 deg
	Y axis	80 ~ 90 deg	35 ~ 50 deg	65 deg
Height (L3)		29 cm	18 ~ 30 cm	28 cm
Handle (L3-L1)		16 cm	13 ~ 20 cm	18.5 cm
Swing (R)		22 cm	10 ~ 16 cm	18 cm
Output torque		10.83 Nm	small	8.9 Nm
Precision		2250/80 counts/deg	low	1100/65 counts/deg
Bandwidth		100 Hz	low	120 Hz
Interface		PCI	USB、game port	PCI
Control		PC	μ-processor	PC
Price		2000 US	100 US	5000 US

$$G_x(s) = \frac{1}{0.095s^2 + 3.0s + 14.8} \tag{11}$$

$$G_y(s) = \frac{1}{0.086s^2 + 2.9s + 15.7}. \tag{12}$$

The transfer function shows a 3 dB output at about 100 Hz, which is taken as the bandwidth of the developed joystick. With the system identification, the joystick system can then be modeled for control and ready for the employment of the software, discussed in section 3. Table 2 lists the comparison of the developed force-reflection joystick with the commercial ones in their hardware performance, including the workspace, output toque, precision, bandwidth, price, *etc*. From the comparison, the SideWinder Force Feedback Pro, manufactured by the Microsoft mainly for entertainment purpose, is cheap, but not accurate. Since its actions are usually in fixed patterns, for instance, shaking in car crash or gun-firing, it is not suitable for bilateral interaction. By contrast, the Immersion Engine 2000 from the Immersion Corporation offers high precision and flexibility in manipulation and control with a much higher price. Meanwhile, the developed force-reflection joystick also achieves comparable bandwidth, precision, and output torque at a lower price.

3. SOFTWARE DEVELOPMENT

We develop the software to make the joystick behave like a manipulative device suitable for a given application. In addition, we also build the virtual walls and then the virtual motion constraints that correspond to the requirements of the given application, discussed in section 3.1. During the development, we first let the joystick emulate the three basic physical elements, the spring, damper, and mass. By synthesizing these three basic elements, we can further make it emulate objects with more complex behaviors. Fig. 5 shows the system block diagram when the operator interacts with the environment or

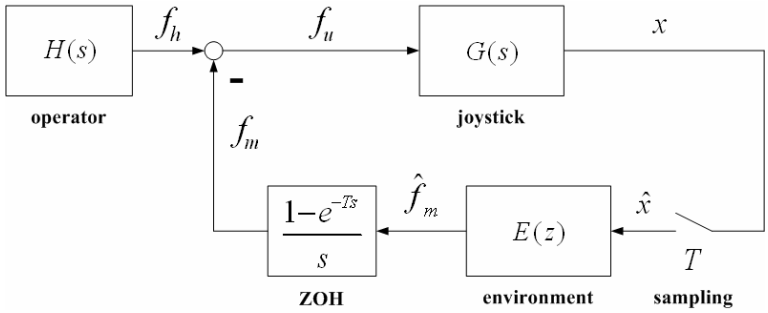

Fig. 5. System block diagram with the operator interacting with the environment to emulate using the force-reflection joystick.

object to emulate using the force-reflection joystick [14]. In Fig. 5, the operator sends in the commanded force f_h and receives the reflection force f_m from the joystick. f_h and f_m, combined to be f_u, are sent to the joystick, represented by $G(s)$, which in turn generates the command x. Via sampling, the command $\hat{x}$ is sent to $E(z)$, which stands for the environment or object to emulate. The interactive force $\hat{f}_m$, becoming f_m after the zero order hold (ZOH), is then sent back to the operator. Through the process, the operator may feel like manipulating the emulated device or object when she/he is actually manipulating the joystick.

To achieve successful emulation, system stability under digital implementation needs to be ensured. For this stability analysis, we adopt the passivity condition for sampled data systems derived in [15] below:

$$b > \frac{T}{2} \cdot \frac{1}{1-\cos \omega T} \cdot Re\{(1-e^{-j\omega T}) \cdot E(e^{j\omega T})\} \tag{13}$$

where b is the damping term of the transfer function of the joystick, described in Eq. (8), and $0 \le \omega \le \omega_N$, $\omega_N = \pi/T$, the Nyquist frequency. By applying Eq. (13) for spring emulation ($F = Kx$, *i.e.*, $E(z) = K$), we can obtain

$$K < \frac{2b}{T}. \tag{14}$$

With Eq. (14) and the maximum updating frequency of the system at 100 Hz, the values of K in the X and Y directions need to be smaller than 605 and 566 N/m, respectively, for the virtual spring to be stable. For damper emulation ($F = Bv$, *i.e.*, $E(z) = B \cdot (z - 1)/Tz$), we can obtain

$$B < \left| \frac{b}{\cos \omega T} \right|. \tag{15}$$

In Eq. (15), the minimum value in the right side occurs at $\omega = 0$ or $\omega = \omega_N$. Thus, Eq. (15) is rewritten as

$$B < b. \tag{16}$$

From Eq. (16), the values of B in the X and Y directions need to be smaller than 3.0 and 2.9 N·s/m, respectively, for the virtual damper to be stable. As for mass emulation ($F = Ma$, *i.e.*, $E(z) = M \cdot [(z-1)/Tz]^2$), we can obtain

$$M < \left| \frac{bT}{\cos 2\omega T - \cos \omega T} \right|. \tag{17}$$

In Eq. (17), the minimum value in the right side occurs at $\omega = \omega_N$. Thus, Eq. (17) is rewritten as

$$M < \frac{bT}{2}. \tag{18}$$

From Eq. (18), the values of M in the X and Y directions need to be smaller than 0.015 and 0.014 kg, respectively, for the virtual mass to be stable. By combining the spring, damper, and mass as an impedance [16], a more complex object can be synthesized, with its model described in Eq. (19) and passivity condition in Eq. (20):

$$E(z) = K + B \cdot \frac{z-1}{Tz} + M \cdot \left(\frac{z-1}{Tz} \right)^2 \tag{19}$$

$$\frac{KT}{2} + B + \frac{2M}{T} < b. \tag{20}$$

For the virtual impedance to be stable, the parameters in Eq. (20) need to satisfy the constraints described in Eq. (21):

$$\begin{bmatrix} K_x + 200B_x + 200^2 M_x \\ K_y + 200B_y + 200^2 M_y \end{bmatrix} < \begin{bmatrix} 605 \\ 566 \end{bmatrix} \tag{21}$$

where M_x, M_y, B_x, B_y, K_x, and K_y are the components of M, B, and K in the X and Y directions, respectively. A series of experiments have been performed to emulate the spring, damper, mass, and impedance. The parameters in the emulation were selected to satisfy the constraints specified in Eqs. (14) to (21). Emulations conducted involve both single and two joints of the joystick. From the measured position and force responses, the joystick well emulated these objects. The system was stable and only insignificant coupling effects between the two joints were observed. Note that unsmooth motions were observed in damper emulation when the joystick moved with high velocities. It was because the discontinuous variation in the resistant force due to fast-varying velocity and damping effect would yield the operator an unnatural feeling, thus leading to a not so smooth motion. By contrast, force generation in spring emulation was much smoother for involving mainly the position data.

3.1 Virtual Wall and Motion Constraint

With the joystick capable of emulating the basic physical elements, we then let it emulate the behavior of interacting with a virtual wall. Accordingly, a set of horizontal

and vertical walls will be built. These walls will serve as the building blocks for constructing the virtual motion constraints corresponding to the given task requirements. In assembling the walls, we need to consider the connection between the horizontal and vertical walls and a smooth transition between them. Salient cruising can thus be achieved when the joystick moves between walls or takes turns.

The implementation of the virtual wall poses the difficulty in demanding a very high stiffness for the wall itself and exhibiting an abrupt stiffness change during contact with the wall, as shown in Fig. 6 (a). In Fig. 6 (a), the force imposed on the wall f_{act} should be equal to the reactive force f_{rea} at the moment of contact, when a virtual wall is very stiff. In practice, Colgate *et al*. suggest the stiffness of the virtual wall to be as high as 2000 ~ 8000 N/m [17]. Minsky *et al*. suggest the following formula to be satisfied [18]:

$$\frac{B}{K \cdot T} > C \approx 0.5. \tag{22}$$

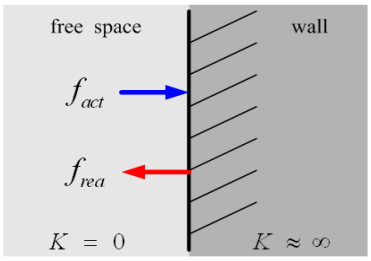

Fig. 6. (a) Conceptual diagram of a virtual wall.

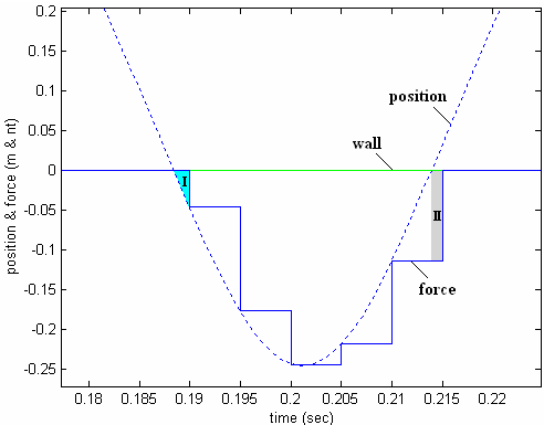

Fig. 6. (b) The phenomenon of deferred force generation when the joystick is pushing into the wall.

In addition to the challenge in achieving high stiffness, digital implementation of the virtual wall may also incur the problem of deferred force generation [17]. Fig. 6 (b) shows the phenomenon of deferred force generation when the joystick is pushing into a virtual wall. This simulation illustrates how the speed of the joystick and the system sampling rate may affect the implementation. In the simulation, the sampling rate was set to be 200 Hz, and the relation between the distance pushed into the wall x and the corresponding reflective force f formulated as $f = g \cdot x$, where g stands for the stiffness. To simplify the illustration, g was chosen to be 1, such that both the position and force were with the same scale and could be overlapping in the figure. In Fig. 6 (b), the joystick entered the wall at 188 ms, while the simulated reflective force was computed until 190 ms, resulting in late energy generation specified in region I. Similarly, when the joystick left the wall at 213 ms, the force was computed until 215 ms, resulting in another late energy generation specified in region II. This late response might invoke system instability and yield the human operator the unnatural response. From Fig. 6 (b), a larger sampling rate can decrease the widths of regions I and II, and a smaller joystick speed decrease their

heights. To yield the human operator an instant reflective force, it may demand a sampling rate up to 1 K Hz [19].

To tackle these problems aforementioned, under the limitations of the sampling rate of the developed joystick, our strategy is to constrain the speed of the joystick. Therefore, we design the virtual motion constraints using pairs of walls, which form aisles and constrain the joystick to move within them slowly. Another issue in the design is about the pushing force a human operator may impose on the joystick. According to [20], a human may generate a pushing force up to more than 60 N. If the operator keeps pushing against the joystick with the maximum force, the push may bend the joystick and make the virtual wall collapse. While the human operator is expected not to push hard on the wall intentionally, the system will send out a sound warning when a very large pushing force occurs. In addition, based on the concept of pseudo-haptic feedback [21], we utilize the visual illusion to provide an extra resistive force for the joystick. The idea is to retain the image of the joystick within the aisle, even though the imposed force has actually pushed the joystick outside of the aisle. This visual illusion was proved to be useful, when the real and virtual feeling were not that much different. The experiments shown later also demonstrate that the pseudo-haptic feedback did make the operator experience a much stiffer wall than it actually was.

In implementing the wall, we set the stiffness to be around 5000 N/m. With so high a stiffness, the constraint for the passivity condition, specified in Eq. (21), is violated. We tested system performance under such condition, and found the joystick might bounce between the walls when it hit the wall hard. The oscillation phenomenon could be alleviated with the operator's hand resting on the joystick, as certain resistive force was provided. This resistive force could also be generated by introducing the damping into the virtual wall, which had acted like a pure spring originally. With both speed reduction of the joystick and damping incorporated in the virtual wall, this virtual wall emulation exhibited stability under a violated passivity condition.

4. EXPERIMENTS

As a demonstration, we used a set of virtual walls to build a virtual manual gearshift system, and checked whether the developed 2-DOF force-reflection joystick would behave like a gearshift lever. Fig. 7 (a) shows the developed virtual manual 5-speed gearshift system, which consists of one horizontal and three vertical aisles, formed by eight pairs of virtual walls, shown in Fig. 7 (b). These aisles confine the region for the joystick to move within. The five speed gear positions and that for the reverse gear are located at the two ends of the three vertical aisles, marked by 1 to 5 and R, respectively. Three junctions are formed at the intersections between the horizontal and vertical aisles, marked by I, II, and III, respectively, and their enlarged views are shown in Fig. 7(c). Junctions I and III are with one side of the junction closed, and junction II is open in all four directions. To prevent the joystick from penetrating into the closed end of the aisle for the cases of junctions I and III, we have designed a rectangular buffer region, enclosed by the white line, shown in Fig. 7 (c). When the joystick enters the buffer region, the force from the vertical direction is generated and deviates it into the vertical aisle. Our design also includes a locking function when the joystick rests in the six gear positions,

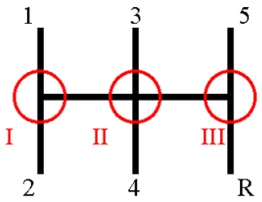

(a) A virtual manual 5-speed gearshift system.

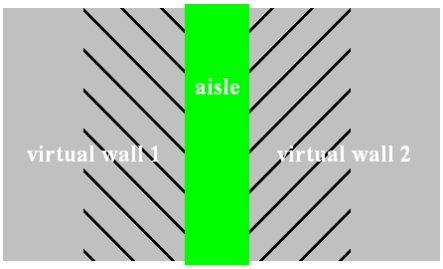

(b) An aisle formed by two virtual walls.

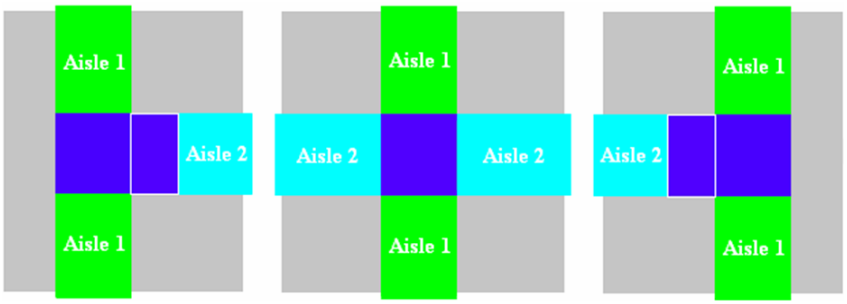

(I) (II) (III)

(c) Three types of aisle junctions.

Fig. 7. Construction of a virtual manual gearshift system.

and an automatic return to the neutral position, located at junction II, when the joystick is away from the gear positions.

With the virtual manual gearshift system built, we then executed experiments to evaluate its performance. We started with its building block, the virtual wall. Refer to Fig. 6 (a), Fig. 8 shows the emulation result when the joystick was pushed into and then pulled out of the virtual wall. Fig. 8 (a) shows one typical position trajectory of the joystick during the process, in which the joystick moved from the free space (negative coordinate), made contact with the wall, entered the wall (positive coordinate), and then moved out. From the position trajectory of the joystick and the preset impedance of the virtual wall, the reflective force from the virtual wall was computed and fed back to the operator's hand via the joystick. This reflective force, resisted by the hand, was then measured by the force sensor equipped on the joystick, as shown in Fig. 8 (b). From Fig. 8, the force response did reflect the penetration of the joystick into the wall. And, most of the operators conducting the experiments reported a feeling of contacting with a stiff wall.

We went on to evaluate the performance of the entire virtual manual gearshift system. Refer to Fig. 7 (a), Fig. 9 shows the emulation result when the operator manipulated the virtual gearshift lever to pass through the six gear positions. Fig. 9 (a) shows one typical position trajectory of the virtual gearshift lever during the process, in which the lever started from the neutral position, moved to the five speed gear positions, and finally reached the reverse gear position. Fig. 9 (b) shows the corresponding force response measured by the force sensor, which reflected how the joystick hit the wall during the movement. During the manipulation, the lever was confined to move within the aisles.

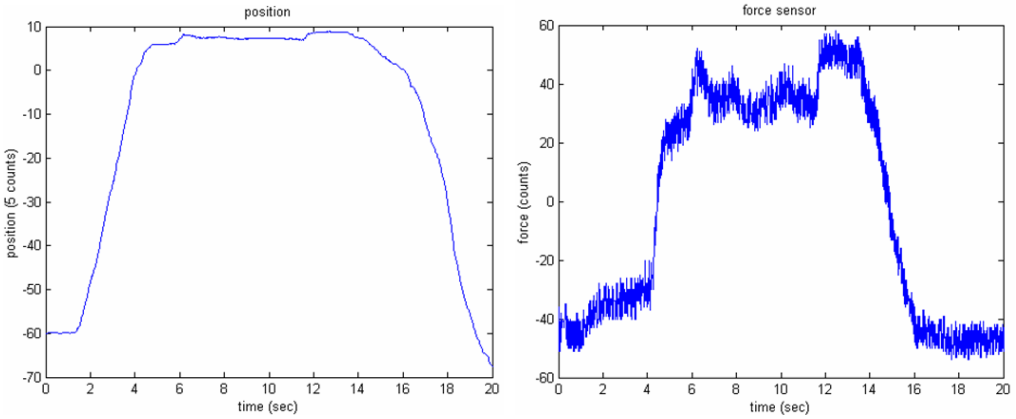

(a) Position trajectory of the joystick. (b) Measured force response from the force sensor.

Fig. 8. Results for virtual wall emulation.

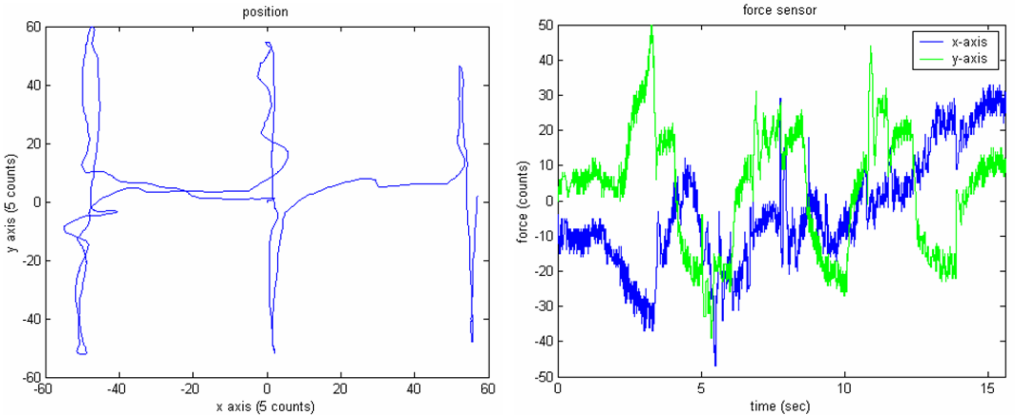

(a) Position trajectory of the gearshift lever. (b) Measured force response from the force sensor.

Fig. 9. Results for virtual gearshift emulation.

And, most of the operators reported that the virtual constraints did provide them the guidance and they experienced a realistic feeling of interacting with a real manual gearshift system.

5. CONCLUSION

In this paper, we have developed a force-reflection joystick system for VR simulation. To make it fit for various applications, virtual motion constraints have been constructed based on using a set of virtual walls. In experiments, a virtual manual gearshift system has been built to demonstrate the capability of the developed system. This system can also be used to emulate various kinds of manipulative devices by properly assembling the virtual walls. In future works, we will enhance its hardware and software, so that more realistic and versatile virtual walls can be built. A systematic approach for vir-

tual wall assembly will also be developed, so that virtual motion constraints for a given application can be constructed autonomously.

REFERENCES

1. C. C. P. Chu, T. H. Dani, and R. Gadh, "Multimodal interface for a virtual reality based computer aided designed system," in *Proceedings of IEEE International Conference on Robotics and Automation*, 1997, pp. 1329-1334.
2. C. L. Clover, G. R. Luecke, J. J. Troy, and W. A. McNeely, "Dynamic simulation of virtual mechanisms with haptic feedback using industrial robotics equipment," in *Proceedings of IEEE International Conference on Robotics and Automation*, 1997, pp. 724 -730.
3. C. P. Kuan and K. Y. Young, "VR-based teleoperation for robot compliance control," *Journal of Intelligent and Robotic Systems*, Vol. 30, 2001, pp. 377-398.
4. A. Nahvi, D. D. Nelson, J. M. Hollerbach, and D. E. Johnson, "Haptic manipulation of virtual mechanisms from mechanical CAD designs," in *Proceedings of IEEE International Conference on Robotics and Automation*, 1998, pp. 375-380.
5. F. Vahora, B. Temkin, T. M. Krummel, and P. J. Golman, "Development of real-time reality haptic application: real-time issues," in *Proceedings of the 12th IEEE Symposium on Computer-Based Medical Systems*, 1999, pp. 290-295.
6. G. Burdea, *Force and Touch Feedback for Virtual Reality*, John Wiley and Sons, New York, 1996.
7. L. Joly and C. Andriot, "Imposing motion constraints to a force reflecting telerobot through real-time simulation of virtual mechanisms," in *Proceedings of IEEE International Conference on Robotics and Automation*, 1995, pp. 357-362.
8. L. B. Rosenberg, "Virtual fixtures: perceptual tools for telerobotic manipulation," in *Proceedings of IEEE Virtual Reality Annual International Symposium*, 1993, pp. 76-82.
9. H. Kazerooni and M. G. Her, "The dynamics and control of a haptic interface device," *IEEE Transactions on Robotics and Automation*, Vol. 10, 1994, pp. 453-464.
10. M. Ouhyoung, W. N. Tsai, M. C. Tsai, J. R. Wu, C. H. Huang, and T. J. Yang, "A low-cost force feedback joystick and its use in PC video games," *IEEE Transactions on Consumer Electronics*, Vol. 41, 1995, pp. 787-794.
11. A. Frisoli, C. A. Avizzano, and M. Bergamasco, "Simulation of a manual gearshift with a 2 DOF force-feedback joystick," in *Proceedings of IEEE International Conference on Robotics and Automation*, 2001, pp. 1364-1369.
12. B. D. Adelstein and M. J. Rosen, "Design and implementation of a force reflecting manipulandum for manual control research," in *Advances in Robotics*, H. Kazerooni, ed., ASME Winter Annual Meeting, 1992, pp. 1-12.
13. L. Ljung, *System Identification: Theory for the User*, 2nd ed., Prentice Hall, 1998.
14. R. J. Adams and B. Hannaford, "Control law design for haptic interfaces to virtual reality," *IEEE Transactions on Control Systems Technology*, Vol. 10, 2002, pp. 3-13.
15. J. E. Colgate and G. Schenkel, "Passivity of a class of sampled-data systems: application to haptic interfaces," *Journal of Robotic Systems*, Vol. 14, 1997, pp. 37-47.
16. N. Hogan, "Impedance control: an approach to manipulation," *ASME Transactions*,

Journal of Dynamic Systems, Measurement, and Control, Vol. 10, 1985, pp. 1-24.
17. J. E. Colgate, P. E. Grafing, M. C. Stanley, and G. Schenkel, "Implementation of stiff virtual walls in force-reflecting interfaces," in *Proceedings of IEEE Virtual Reality Annual International Symposium*, 1993, pp. 202-208.
18. M. Minsky, M. Ouhyoung, O. Steele, F. P. Brooks, Jr., and M. Behensky, "Feeling and seeing: issues in force display," *Computer Graphics*, Vol. 24, 1990, pp. 235-243.
19. Y. Adachi, T. Kumano, and K. Ogino, "Intermediate representation for stiff virtual objects," in *Proceedings of IEEE Virtual Reality Annual International Symposium*, 1995, pp. 203-211.
20. A. R. Tilley, *The Measure of Man and Woman – Human Factors in Design*, Henry Dreyfuss Associates, John Wiley and Sons, New York, 2002.
21. A. Lecuyer, S. Coquillart, A. Kheddar, P. Richard, and P. Coiffet, "Pseudo-haptic feedback: can isometric input devices simulate force feedback?" in *Proceedings of IEEE Virtual Reality*, 2000, pp. 83-90.

Wei-Ching Lin (林瑋慶) was born in Tucheng, Taiwan, 1977. He received his B.S. degree in Electrical Engineering from National Taiwan University of Science and Technology, Taiwan, in 2000, and M.S. degree in Electrical and Control Engineering from National Chiao Tung University, Hsinchu, Taiwan, in 2002. Since 2002, he has been with Chung-shan Institute of Science and Technology, Taoyuan, Taiwan. His research interests include robotics, human machine interface, and real-time programming.

Kuu-Young Young (楊谷洋) was born in Kaohsiung, Taiwan, on Dec. 22, 1961. He received his B.S. degree in Electrical Engineering from National Taiwan University, Taiwan, in 1983, and M.S. and Ph.D. degrees in Electrical Engineering from Northwestern University, Evanston, IL, U.S.A., in 1987 and 1990, respectively. Between 1983 and 1985, he served as an electronic officer in Taiwan Navy. Since 1990, he has been with the Department of Electrical and Control Engineering at National Chiao Tung University, Hsinchu, Taiwan, where he is currently a Professor. He served as the chairman of the department from 2003 to 2006. His research interests include robot compliance control, robot learning control, robot calibration and path planning, teleoperation, VR/robot integration, biological control, and brain computer interface.